Journal of Applied Biology & Biotechnology Vol. 15(1), pp. 149-160, January-February, 2027
Available online at http://www.jabonline.in
DOI: 10.7324/jabb.2026.325946

Propolis enhances fibroblast wound healing behavior and is associated with upregulation of SOX4 and ROCK1 mRNA expression

Mochamad Heddy Herdiman[1], Adelina Khristiani Rahayu[2*], Julia Windi Gunadi[3,4]

[1]Department of Anatomy, Faculty of Medicine, Maranatha Christian University, Bandung, Indonesia.
[2]Biotechnology Program Study, Faculty of Medicine, Maranatha Christian University, Bandung, Indonesia.
[3]Master Program of Skin Ageing and Aesthetic Medicine, Faculty of Medicine, Maranatha Christian University, Bandung, Indonesia.
[4]Department of Physiology, Faculty of Medicine, Maranatha Christian University, Bandung, Indonesia.

ARTICLE INFO

Article history:
Received on: 28/06/2026
Accepted on: 08/09/2026
Available Online: 25/11/2026

Key words:
Cell cycle, propolis, ROCK1, SOX4, viability, wound closure

ABSTRACT

Propolis from stingless bees (*Trigona* sp.) has been traditionally used to facilitate tissue regeneration; however, its molecular mechanisms in human dermal fibroblast models remain poorly defined. This study investigated the effects of *Trigona* sp. propolis on fibroblast wound-healing behavior and the associated transcriptional responses of SOX4 and ROCK1. Antioxidant activity was assessed via 2,2-diphenyl-1-picrylhydrazyl radical-scavenging activity, and the chemical profile was characterized by high-performance liquid chromatography (HPLC). Cytotoxicity and cell viability were evaluated in 1306 fibroblast cells using the MTT assay. Wound closure was assessed by an *in vitro* scratch assay, cell cycle distribution by flow cytometry, and SOX4/ROCK1 gene expression by reverse transcriptase–quantitative real-time PCR. Propolis exhibited moderate antioxidant activity (IC_{50} = 51.08 µg/ml), with HPLC tentatively indicating quercetin as a constituent on the basis of retention-time matching. Treatment with 20 µg/ml propolis significantly increased cell viability and accelerated G0/G1-to-S-phase cell cycle transition. Propolis also accelerated wound closure, reaching 96.8% within 24 hours. These phenotypic changes were accompanied by significant upregulation of SOX4 and ROCK1, genes reported to regulate cell cycle progression and cytoskeletal reorganization, respectively. These findings indicate that propolis enhances fibroblast viability, S-phase entry and wound closure, phenotypic changes that were accompanied by upregulation of SOX4 and ROCK1 transcripts, supporting its potential as a natural therapeutic agent for wound healing and warranting further functional validation of the SOX4/ROCK1 axis.

1. INTRODUCTION

Impaired wound healing is a hallmark of numerous pathological and physiological conditions, including aging, vascular insufficiency, burns, and chronic inflammatory disorders, with diabetes representing one well-characterized clinical example [1]. The incidence of diabetes mellitus (DM), a widespread metabolic condition marked by persistent hyperglycemia due to insufficient insulin production, action, or both, is expanding worldwide annually. Data from the International Diabetes Federation indicate a diabetes prevalence of 11.3%, with a total of 20,426,400 adult cases out of a total adult population of 185,217,400 in Indonesia. Globally, these numbers are projected to reach 783 million individuals by the year 2045 [2]. Diabetes mellitus causes pathological changes that impede the healing of wounds, such as vascular, neuropathic, immune system, and metabolic changes [3]. Impaired wound healing can lead to complications in diabetic patients by predisposing them to infections [4]. This emphasizes the importance of the wound-healing process.

Wound healing is a dynamic process comprising hemostasis, inflammation, proliferation, and remodeling, in which fibroblasts play a pivotal role [1,5]. During wound repair, fibroblasts facilitate multiple functions, from the development of connective tissue at the site of damage to secreting signals that attract innate immune cells [6–8]. According to several studies using wound repair models, fibroblasts can migrate to the wound site, exhibit contractile properties, and initiate tissue signaling cascades [9,10]. Among these, SOX4, a transcription factor belonging to the SRY-box family, has been linked to the promotion of fibroblast cell cycle progression from G0/G1 to S phase, while ROCK1 (Rho-associated coiled-coil kinase 1) controls the production of actin stress fibers and directed cell migration. SOX4 is a high mobility group (HMG)-box transcription factor with a well-established, though largely cancer-derived, role as a positive regulator of the G0/G1-to-S-phase cell cycle transition; in cervical cancer cells, SOX4 overexpression accelerated cell cycle progression and proliferation, while its knockdown slowed both [11]. Although this mechanism has not been directly characterized in

*Corresponding Author
Adelina Khristiani Rahayu, Biotechnology Program Study, Faculty of Medicine, Maranatha Christian University, Bandung, Indonesia.
E-mail: adelina.kr @ maranatha.edu

© 2027 Mochamad Heddy Herdiman *et al.* This is an open access article distributed under the terms of the Creative Commons Attribution License -NonCommercial-ShareAlike Unported License (http://creativecommons.org/licenses/by-nc-sa/3.0/).

dermal fibroblasts, the G0/G1-to-S transition SOX4 promotes is the same phenotypic shift required for fibroblast expansion during the proliferative phase of wound healing, making it a plausible, testable candidate regulator in this context. ROCK1, a downstream effector of RhoA/RhoC signaling, phosphorylates myosin light chain to drive actomyosin contractility, a process directly implicated in fibroblast-mediated wound closure; ROCK1-dependent contractility has been demonstrated in primary human lung fibroblasts, in which the ROCK inhibitor Y-27632 dose-dependently reduced collagen gel contraction [12]. Together, SOX4 and ROCK1 represent two biologically distinct but complementary axes relevant to wound repair, namely, cell cycle re-entry and cytoskeletal-driven contractility/migration, respectively. Therefore, the SOX4/ROCK1 axis may represent an important molecular determinant of fibroblast-driven wound repair in general, and its dysregulation has been proposed to contribute to impaired healing in pathological contexts such as diabetes; however, how this pathway responds to natural therapeutic compounds remains poorly understood.

The antibacterial, antioxidant, and anti-inflammatory qualities of propolis, a complex resinous material made by bees by combining plant-derived sap with salivary enzymes, have been thoroughly studied [7,13]. It is a promising option for wound-healing applications due to its high flavonoid content, especially quercetin and kaempferol [14]. Studies conducted *in vivo* have produced strong proof of propolis's effectiveness: Ernawati et al. [15] reported that topical propolis application significantly increased fibroblast growth factor-2 expression and fibroblast numbers in the traumatic ulcers of diabetic rats, whereas Sungkar et al. [16] showed that propolis accelerates wound healing in rats through increased VEGF expression and suppression of NF-κB and caspase-3. Furthermore, propolis has been shown to activate the TGF-β/Smad2,3 transcriptional pathway and promote collagen formation in a diabetic mouse wound model [17]. All these *in vivo* results demonstrate propolis's biological activity as a wound-healing agent; nevertheless, the cellular and molecular mechanisms behind these actions are still poorly known, especially when it comes to the biology of human dermal fibroblasts.

Crucially, as fibroblast gene expression profiles, cell cycle dynamics, and cytoskeletal regulatory mechanisms vary significantly between species, extrapolation from rat *in vivo* models to human clinical application requires mechanistic validation in human cell-based systems [18]. Additionally, the chemistry and plant origin of stingless bee propolis (*Trigona* sp.) have been reviewed in detail [19], yet little is known about its molecular effects on the behavior of human fibroblasts or the gene regulatory networks it interacts with. Specifically, it has not been previously studied whether *Trigona* sp. propolis may act on the SOX4/ROCK1 axis, which has been linked to fibroblast migration and cell cycle progression, two processes relevant to wound re-epithelialization. In addition to confirming propolis's translational potential from animal models to human treatments, closing this mechanistic gap is crucial for pinpointing the precise molecular targets that propolis bioactives, such as quercetin, use to promote regeneration. With an emphasis on cell viability, wound closure, cell cycle progression, and the transcriptional regulation of SOX4 and ROCK1 as candidate molecular correlates of propolis-induced fibroblast activation, this study used the 1306 human skin fibroblast line, a non-malignant dermal fibroblast line immortalized by SV40 transformation, as a foundational in vitro model to examine the effects of *Trigona* sp. propolis on human dermal fibroblast wound-healing behavior.

2. MATERIALS AND METHODS

2.1. Research Design

The experimental work was conducted at the Maranatha Biomedical Research Laboratory (MBRL), Maranatha Christian University. The study was carried out over a seven-month period, spanning from June to December 2025.

2.2. Propolis Extraction

Trigona sp. raw propolis (500 g) was purchased from a commercial supplier (Rahmi Propolis, West Java, Indonesia) and extracted according to the method described by Tan and Rahayu [20]. The sample was dissolved in 70% ethanol (1:2 ratio) and homogenized. The mixture underwent maceration with continuous agitation, where the solvent was filtered and renewed daily for 3 weeks until exhaustive extraction was achieved (indicated by a clear filtrate). The resulting extract was subsequently oven-dried to obtain propolis powder [20].

2.3. 2,2-Diphenyl-1-picrylhydrazyl assay

The free-radical-scavenging capacity was assessed via a 2,2-diphenyl-1-picrylhydrazyl (DPPH) assay adapted from a previously described method [21]. Briefly, 750 µl of propolis extract (3.9; 7.8; 15.6; 31.25; 62.5; 125 µg/ml) was reacted with an equal volume of 0.1 mM DPPH solution. Absorbance was subsequently measured at 517 nm. The percentage of radical inhibition was determined using the following equation:

$$\%\ Inhibition = \frac{Abs_{control} - Abs_{sample}}{Abs_{control}} \times 100$$

2.4. High-Performance Liquid Chromatography (HPLC) Assay

The HPLC analysis specifically focused on the quantification of Quercetin as a representative flavonoid marker. Quercetin standard solutions at concentrations of 20, 40, 60, 80, and 100 ppm were used to create a five-point calibration curve. A 1-mg aliquot of propolis sample was dissolved in 1 ml of HPLC-grade ethanol, injected into the chromatographic system after being filtered using a 0.45 µm membrane. Chromatographic separation was performed on a LiChroCART C-18 column (150 × 4.6 mm, 5-µm particle size) using an isocratic mobile phase of acetonitrile and water (40:60, v/v) at a flow rate of 1 ml/minute, with UV detection at 370 nm and an injection volume of 20 µl. This analysis was targeted specifically at quercetin as a representative flavonoid marker, consistent with the reference method used [20]; it was not intended as a comprehensive phytochemical profile, and other bioactive constituents commonly reported in propolis (e.g., pinocembrin, galangin, and chrysin) were not evaluated in the present study. The identification of quercetin in the propolis extract was determined by matching the retention time of the sample peak with that of the authentic quercetin standard [21,22].

2.5. Cell Culture and Maintenance

The evaluation of cytotoxic activity, cell viability, wound closure, cell cycle distribution, and gene expression was conducted using the 1306 human skin fibroblast cell line. The 1306 human skin fibroblast cell line (Catalogue number 90011887) was obtained from the European Collection of Authenticated Cell Cultures (ECACC, Salisbury, UK). According to the ECACC catalogue, this line is an HPRT-deficient derivative of GM0637, a non-malignant human skin fibroblast line immortalized by SV40 transformation. Cells were maintained in T-25

culture flasks containing growth medium (DMEM supplemented with 10% Fetal Bovine Serum and 1% antibiotic-antimycotic). The medium was replenished every 2 days. All experiments were performed using cells at passage 29.

2.6. Cytotoxicity Assay

To assess cytotoxicity, 2×10^4 cells/well were plated in 96-well plates. Following a PBS wash [23], the cells were exposed to 100 µl of growth medium containing various concentrations of propolis (20–100 µg/ml). A solvent control (0.5% DMSO) and a negative control (cells maintained in growth medium alone) were included for comparison. Each experimental condition was performed in three independent biological replicates ($n = 3$), i.e., three separate experiments performed on different occasions using independently cultured cells.

2.7. Cell viability Assay

Cell viability assays were performed on cells seeded at a density of 20,000 cells/well. After 24 hours of stabilization, the medium was replaced with growth media containing either 0.0625% DMSO or 20 µg/ml propolis (final DMSO concentration 0.0625%). At 24 and 48 hours after treatment, following a PBS wash, the cells were incubated for 4 hours with 100 µl of MTT solution (Roche). After dissolving the formazan precipitates, absorbance was quantified at 595 nm [23,24]. Each experimental condition was performed in three independent biological replicates ($n = 3$), i.e., three separate experiments performed on different occasions using independently cultured cells. MTT absorbance values were expressed as a percentage of the 24-hour negative control, which was set to 100%; values at both 24 and 48 hours were normalized to this single reference, so the 48-hour negative control is not fixed at 100%.

2.8. Wound Closure (scratch assay)

The scratch assay was performed to assess wound closure [23]. Fibroblasts were cultured in 24-well plates (1.5×10^5 cells/well) until 90% confluence was achieved. A linear wound was created across the cell layer using a sterile 200 µl pipette tip. The remaining cells were incubated with either untreated growth medium (negative control) or medium supplemented with 20 µg/ml of propolis extract (final DMSO concentration 0.0625%). Each treatment was conducted as a single experiment with three replicate wells ($n = 3$ technical replicates). Wound closure was observed at 24 and 48 hours after wounding to evaluate wound closure capacity. The calculation of wound closure (%) was done using the formula [23]:

$$\% \, Wound \, Closure = \frac{W_0 - W_t}{W_0} \times 100$$

2.9. Cell Cycle Distribution Analysis

Fibroblasts were seeded into 12-well plates (1.5×10^4 cells/well) in 1 ml of medium. Following attachment, cells were treated with growth medium containing 20 µg/ml propolis (final DMSO concentration 0.0625%). Negative control (cells maintained in growth medium alone) and positive control (insulin-treated cells, 1 IU/ml) were included for comparison. Each experimental condition was performed as a single experiment with three replicate wells ($n = 3$ technical replicates). The cells were then extracted by trypsinization, fixed for 3 hours with 70% ethanol, and centrifuged. Before flow cytometry analysis, the cell pellets were resuspended in Muse® Cell Cycle reagent and incubated for 30 minutes at room temperature in the dark. Cell cycle distribution was determined by gating on the DNA content histogram to define the G0/G1, S, and G2/M regions, with a total of approximately 10,000 events acquired per sample.

2.10. Gene expression Analysis

The quantification of mRNA expression levels was conducted using reverse transcriptase–quantitative real-time PCR [23]. The experimental setup included a negative control group (cells maintained in growth medium alone), a solvent control group (0.0625% DMSO), and a propolis-treated group (20 µg/ml propolis, final DMSO concentration 0.0625%), with all performed in three independent biological replicates ($n = 3$), i.e., three separate experiments performed on different occasions using independently cultured cells, with each measured in technical triplicate qPCR reactions. Following a 48-hour incubation, total RNA was isolated using GENEzol™ Reagent. RNA purity and concentration were assessed spectrophotometrically, with A260/280 ratios of 1.9–2 considered acceptable for downstream analysis. Subsequently, cDNA synthesis was carried out using the ReverTra Ace™ RT Master Mix kit. For the qPCR step, amplification was performed using THUNDERBIRD™ Next SYBR qPCR Mix with specific primers for SOX4, ROCK1, and GAPDH (Table 1), as described in our previous study [23]. The reaction was run with an annealing temperature of 60°C. Primer efficiencies were determined using serial dilutions of pooled cDNA, yielding efficiencies of 100.7% for SOX4 (slope = −3.304, $R^2 = 0.9869$), 109.6% for GAPDH (slope = −3.111, $R^2 = 0.9802$), and 107.0% for ROCK1 (slope = −3.164, $R^2 = 0.9956$), all within the acceptable 90%–110% range. The dilution series spanned 0.05–500 ng for SOX4 and GAPDH and 100–500 ng for ROCK1. Melt curve data were not available for analysis in the present study. Both no-template and no-reverse-transcriptase controls yielded no detectable Cq value, confirming the absence of reagent contamination and genomic DNA carryover, respectively.

2.11. Statistics

All statistical analyses were performed using GraphPad Prism, version 9. Prior to hypothesis testing, normality of each dataset was assessed using the Shapiro–Wilk test. For cytotoxicity data, one-way analysis of variance (ANOVA) with Dunnett's post-hoc test was used to compare the negative control against the solvent control and each propolis concentration (20–100 µg/ml); normality was met across all groups (all $p > 0.05$), and variance homogeneity was confirmed (Brown–Forsythe test: $F(6,14) = 0.805$, $p = 0.5825$). For viability data, two-way ANOVA was applied with matching restricted to treatment groups within each independent experimental batch (column subjects), as viability measurements at 24 and 48 hours were obtained from separate, non-paired wells due to the destructive nature of the MTT assay, followed by Tukey's post-hoc test. Normality was confirmed for five of six time × treatment groups (all $p > 0.05$); the 24-hour negative control group could not be evaluated, as all replicate values equaled 100% by normalization convention (zero variance), for which the Shapiro–Wilk

Table 1. Primers used in the study.

Gene	Forward Primers (5'-3')	Reverse Primers (5'-3')
SOX-4	CTGTCGGGTCTCTAGTTCTT	GAATCGGCACTAAGGAGTTG
ROCK-1	ATGTGACTGAGTGCCCTGTG	TGTGCCAAAGCAAGGACAGA
GAPDH	GTTACCAGGGTCGCCTTCTC	GATGGTGATGGGTTTCCCGT

statistic is mathematically undefined. For wound closure data, two-way repeated-measures (RM) ANOVA was applied with matching across both time and treatment factors, reflecting the non-destructive scratch assay design in which the same wound area was imaged repeatedly at 0, 24, and 48 hours, followed by Tukey's post-hoc test. For cell cycle data, two-way RM ANOVA (mixed-effects model, REML, to accommodate missing values) was applied with matching restricted to cell cycle phase (row factor) only, reflecting that the three phases (G0/G1, S, and G2/M) were derived from the same flow cytometry sample, whereas treatment groups corresponded to independent samples; the Geisser-Greenhouse correction was applied (sphericity not assumed), followed by Tukey's post-hoc test. Normality was confirmed for all nine phase × treatment combinations (all $p > 0.05$). For gene expression data (SOX4, ROCK1), one-way ANOVA with Tukey's post-hoc test was used to compare negative control, solvent control, and propolis-treated groups. Normality was confirmed for all groups for both SOX4 and ROCK1 (all $p > 0.05$); variance homogeneity (Brown–Forsythe test) was confirmed for both SOX4 ($F(2,6) = 0.093$, $p = 0.9129$) and ROCK1 ($F(2,6) = 0.069$, $p = 0.9340$). A significance threshold of $p < 0.05$ was applied throughout. Replication differed between assays: the cytotoxicity, cell viability and gene expression assays were performed as three independent biological replicates (separate experiments using independently cultured cells), whereas the scratch (wound closure) and cell cycle assays were performed once, with three replicate wells analyzed within that single experiment. Statistical estimates for the latter two assays therefore reflect within-experiment variability only and should be interpreted with corresponding caution.

3. RESULTS

3.1. Antioxidant Study of Propolis Ethanolic Extracts Using DPPH Assay

The results showed that the propolis ethanolic extract at various concentrations (3.9, 7.8, 15.6, 31.25, 62.5, and 125 µg/ml) exhibited inhibition percentages of −8.5%, −2.2%, 10%, 39%, 63.3%, and 70.2%, respectively. Two graphs were plotted to correlate the sample concentration (and its log values) with the percentage of inhibition, as shown in Figure 1. According to the IC_{50} calculation, 50% of the free radicals may be inhibited at a concentration of 51.08 µg/ml.

3.2. HPLC Results

HPLC analysis revealed that pure quercetin standards (20–100 ppm) exhibited a single dominant peak with a retention time ranging from 2.03 to 2.22 minutes, as shown in Figure 2G. In contrast, the propolis sample displayed a complex profile with multiple peaks at various retention times (Fig. 2F). A comparison of the chromatograms shows that two peaks within the propolis sample, at retention times of 2.14 and 2.22 minutes, fall within the retention-time range established by the quercetin standard series (2.03–2.22 minutes across 20–100 ppm) (Fig. 2 F and G). The 2.14-minute peak was considered the more probable quercetin signal, as it fell within the tighter retention-time cluster formed by the three highest, most internally consistent calibration points (2.12–2.17 minutes at 60–100 ppm), whereas the 2.22-minute peak matched only the most dilute standard (20 ppm), whose retention time itself deviated from this cluster. Back-calculation from the calibration curve ($y = 108649x–374755$, $R^2 = 0.9882$) using the 2.14-minute peak area yielded an estimated quercetin concentration of 39.93 ppm, corresponding to approximately 39.9 mg quercetin/g propolis (3.99% w/w); the alternative assignment (2.22 minutes) yielded 22.51 ppm (22.5 mg/g, 2.25% w/w). Given the reasoning above, the former is considered the more probable estimate. As identification relied on retention-time matching alone, co-elution of structurally related compounds cannot be excluded, and confirmatory analysis (e.g., co-injection/spiking, spectral matching, or LC-MS) would be required to resolve this ambiguity definitively.

3.3. Cell Cytotoxicity

The cell viability assay was conducted using propolis concentrations of 20, 40, 60, 80, and 100 µg/ml. One-way ANOVA revealed a significant effect of propolis concentration on cell viability ($F(6,14) = 263.7$, $p < 0.0001$, $R^2 = 0.9912$), with treatment accounting for 99.12% of the total variation. Dunnett's post-hoc comparisons showed that, compared to the negative control, treatment with 20 µg/ml (131.7%, mean difference = −31.68, 95% CI: −42.14 to −21.21, $p < 0.0001$) and 40 µg/ml (119.9%, mean difference = −19.94, 95% CI: −30.41 to −9.475, $p = 0.0004$) significantly increased viability, while 60 µg/ml (98.43%) showed no significant difference ($p = 0.9947$). In contrast, 80 µg/ml (44.82%, mean difference = 55.18, 95% CI: 44.71 to 65.64, $p < 0.0001$) and 100 µg/ml (16.65%, mean difference = 83.35, 95% CI:

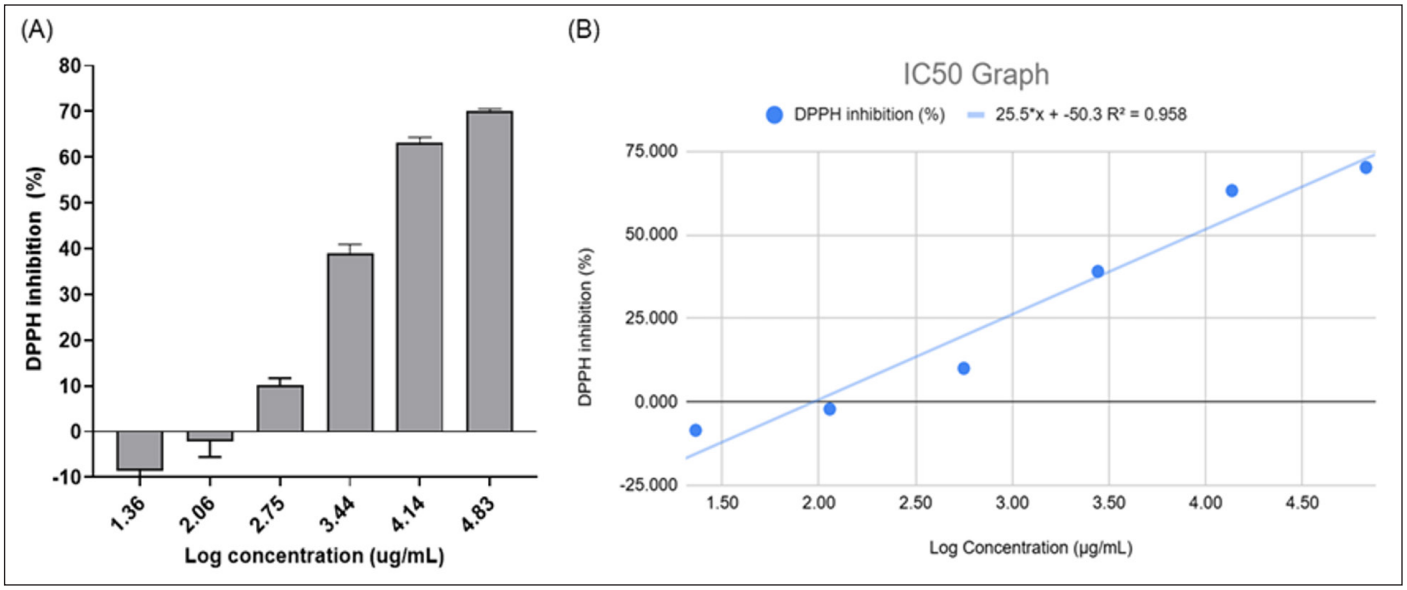

Figure 1. DPPH radical-scavenging activity of propolis ethanolic extract. (A) Percentage (%) of free radical inhibition across various concentrations of propolis. (B) Linear regression graph for the determination of the half-maximal inhibitory concentration (IC_{50}). Data are presented as mean ± SD ($n = 3$).

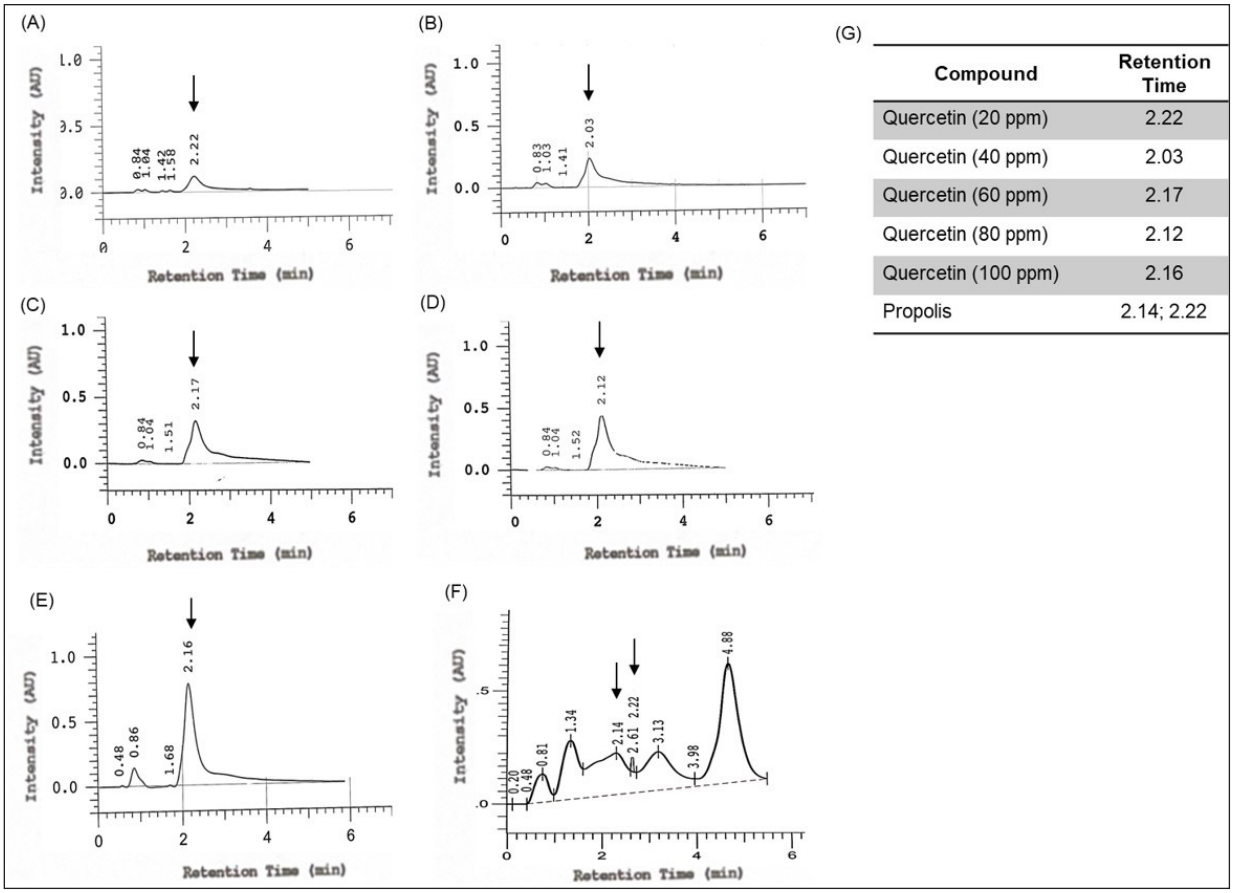

(G)

Compound	Retention Time
Quercetin (20 ppm)	2.22
Quercetin (40 ppm)	2.03
Quercetin (60 ppm)	2.17
Quercetin (80 ppm)	2.12
Quercetin (100 ppm)	2.16
Propolis	2.14; 2.22

Figure 2. Chemical profiling of propolis using High-Performance Liquid Chromatography (HPLC). (A–E) Chromatograms of authentic quercetin standards at concentrations of 20, 40, 60, 80, and 100 ppm, respectively. (F) Representative HPLC chromatogram of the propolis sample, showing two peaks (retention times 2.14 and 2.22 minutes) falling within the retention-time range of the quercetin standard series; assignment is tentative and based on retention-time matching alone. (G) Summary table of retention times (RT) used for this comparison.

72.89 to 93.82, $p < 0.0001$) significantly reduced viability, indicating cytotoxicity at these concentrations. The solvent control did not differ significantly from the negative control (mean difference = 2.743, 95% CI: −7.722 to 13.21, $p = 0.9309$), confirming that the vehicle alone did not affect viability. The results presented in Figure 3 also demonstrated that propolis at concentrations of 80 and 100 µg/ml was toxic to fibroblast cells. This was in line with the decreasing of cell viability to 44.82% and 16.65%, respectively, after 48 hours of treatment compared to the negative and solvent controls. Based on this cytotoxicity profile, the 20 µg/ml concentration, which produced the highest non-toxic increase in viability, was selected for all subsequent functional assays (viability, wound closure, cell cycle, and gene expression); the remaining non-toxic concentration (40 µg/ml) and the toxic concentrations (60–100 µg/ml) were not further evaluated in these functional assays, which is acknowledged as a limitation in the Discussion.

3.4. Cell Viability

The cell viability of 1306 fibroblasts was further monitored over 24 and 48 hours at the selected dose of 20 µg/ml to determine the optimal time-point for achieving confluence, which is a prerequisite for the subsequent wound closure (scratch) assays. As shown in Figure 4, the viability of the fibroblast cell line increased after 24 hours of treatment, reaching 129.6% of the 24-hour negative control. Viability remained elevated at 48 hours, reaching 143.7% on the same scale, at which point the time-matched negative control read 109.8%; the propolis effect at 48 hours therefore corresponds to an increase of approximately 34 percentage points over its own time-matched control. These results indicate that propolis increased the viability of 1306 fibroblast cells. Two-way ANOVA revealed a significant Time × Treatment interaction ($F(2,8) = 13.17$, $p = 0.0029$), accounting for 10.26% of the total variation; the main effects of treatment (84.15% of total variation, $p = 0.0002$) and time (1.69%, $p = 0.0422$) were also significant. Tukey's post-hoc test confirmed that propolis significantly increased cell viability compared to both the negative control and the solvent control at 24 hours (*vs.* negative control: mean difference = −29.60, 95% CI: −40.30 to−18.90, $p < 0.0001$; *vs.* solvent control: mean difference = −21.59, 95% CI: −32.29 to −10.89, $p = 0.0002$) and at 48 hours (*vs.* negative control: mean difference = −33.84, 95% CI: −44.54 to −23.14, $p < 0.0001$; *vs.* solvent control: mean difference = −44.07, 95% CI: −54.77 to −33.37, $p < 0.0001$). The negative and solvent controls did not differ significantly from each other at either time point (24 hours: $p = 0.1942$; 48 hours: $p = 0.0639$), indicating that the vehicle itself did not substantially affect cell viability. Re-analysis showed that cell viability in propolis-treated cells was significantly higher at 48 hours than at 24 hours (mean difference = −14.08, 95% CI: −24.78 to −3.381, $p = 0.0084$), indicating a further, modest increase with prolonged exposure.

3.5. Wound Closure (scratch assay)

Observational data indicated that fibroblast cells underwent wound closure from 0 to 48 hours following treatment with 20 µg/ml propolis (Fig. 5A). Quantitative analysis revealed that the percentage of wound closure reached 96.8% at 24 hours after treatment. By 48 hours,

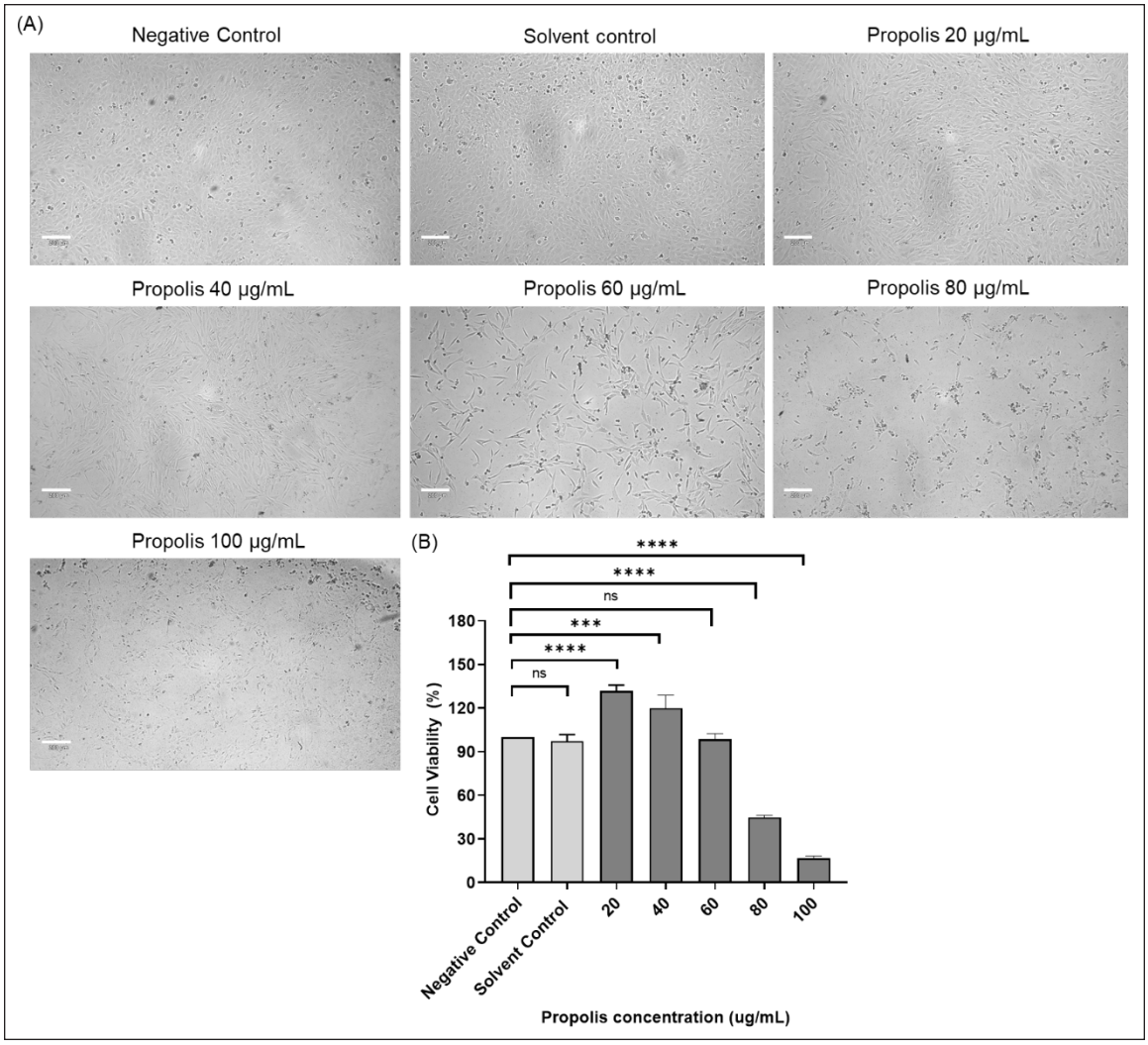

Figure 3. Cytotoxicity of propolis on the 1306 human skin fibroblast cell line after 48 hours. (A) Representative phase-contrast micrographs showing the morphology of 1306 fibroblasts under various treatment concentrations. (B) Quantification of cell viability using the MTT assay. Results are expressed as a percentage relative to the negative control. Data represent mean ± SD (n = 3); ns = not significant; *** $p < 0.001$; **** $p < 0.0001$.

the wound closure increased to 99.7% (Fig. 5B), indicating that the fibroblast monolayer was nearly completely closed. At the 48-hour time point, no significant difference was observed compared to the 24-hour time point or the negative control. This plateau likely occurred because the wound area had reached confluency, leaving no available space for further closure. Furthermore, the results demonstrated that propolis treatment accelerated wound closure compared to the control group. Specifically, the control group exhibited only 71.3% wound closure after 24 hours of incubation and reached 97% after 48 hours. Two-way RM ANOVA revealed a significant Time × Treatment interaction (p = 0.0052), which accounted for 24.22% of the total variation; the main effects of time (38.14% of total variation, p = 0.0015) and treatment (36.94%, p = 0.0038) were also significant. Tukey's post-hoc test confirmed that propolis significantly accelerated wound closure compared to the negative control at 24 hours (mean difference = −25.42, 95% CI: −33.50 to −17.34, p = 0.0053). By 48 hours, wound closure did not differ significantly between propolis and the negative control (mean difference = −2.673, 95% CI: −10.75 to 5.407, p = 0.3380), nor between the 24- and 48-hour propolis time points (mean difference = −2.900, 95% CI: −10.98 to 5.180, p = 0.3006), consistent with near-complete closure in both groups by this time point.

3.6. Cell Cycle Distribution

The results indicated that the cell cycle distribution following treatment with 20 µg/ml propolis showed a significant increase in the number of cells in the S phase compared to the control (as shown in Fig. 6D). The G0/G1 and G2/M phases, on the other hand, did not differ significantly from the cell control and positive control groups. Two-way RM ANOVA (matching within phase, Geisser-Greenhouse corrected) revealed a significant Phase × Treatment interaction ($F(4,12) = 4.968$, p = 0.0135), accounting for 24.72% of the total variation and indicating that the effect of propolis treatment differed across cell cycle phases. There was a significant main effect of phase ($F(1.343, 8.055) = 14.13$, p = 0.0038; 35.16% of total variation), while the main effect of Treatment group did not reach significance (15.07% of total variation; $F(2,6) = 4.459$, p = 0.0651). Tukey's post-hoc comparisons showed that propolis significantly increased the proportion of cells in S phase compared to the negative control (mean difference = −9.167, 95% CI:

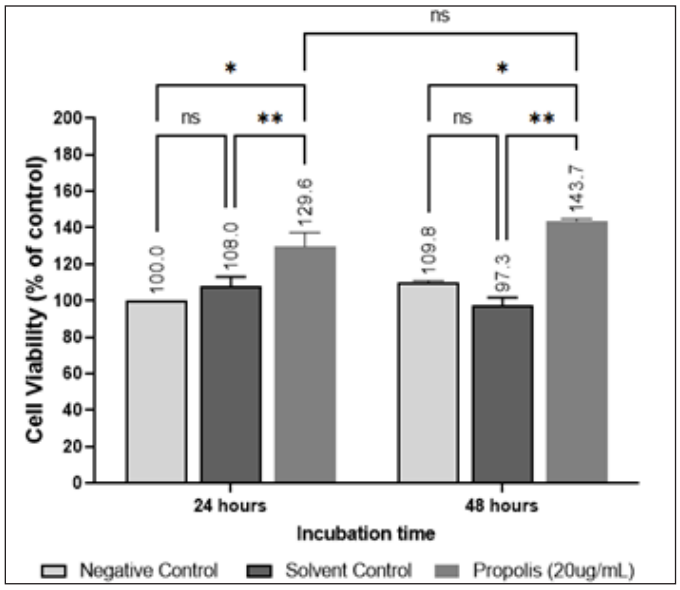

Figure 4. Time-dependent cell viability of 1306 fibroblasts following propolis treatment. Cell viability was assessed by MTT assay after 24 and 48 hours of treatment with 20 µg/ml propolis. All values, including those at 48 hours, were normalized to the 24-hour negative control, which was set to 100%; the 48-hour negative control therefore does not equal 100%. Data are shown as mean ± SD. ns = not significant; * = $p < 0.05$; ** = $p < 0.01$.

−16.06 to −2.272, $p = 0.0200$), while the difference between propolis and the positive control did not reach significance ($p = 0.0790$); no significant differences among groups were observed in the G0/G1 ($p = 0.6441$) or G2/M ($p = 0.8884$) phases. These findings indicate that propolis selectively promotes S-phase entry rather than producing a uniform shift across all cell cycle phases. All comparisons were made against the negative control within the same cell line, and the increase in the S-phase proportion remained statistically significant, indicating that the shift is attributable to propolis treatment rather than to the transformed background of the line. It should be noted, however, that SV40 large T antigen inactivates p53 and retinoblastoma protein function, so the G1/S restriction point in this line is already deregulated; the magnitude of the S-phase response in primary human dermal fibroblasts therefore remains to be determined.

3.7. Relative Expression of Gene Target

The results shown in Figure 7A indicate that the relative expression of the SOX4 mRNA after treatment with propolis was significantly increased 1.70-fold compared to the negative control (cells maintained in growth medium alone). Similarly, Figure 7B demonstrated that the relative expression of the ROCK1 mRNA after treatment with propolis was also significantly increased 2.01-fold, compared to the negative control. One-way ANOVA revealed a significant effect of treatment on SOX4 mRNA expression ($F(2,6) = 9.306$, $p = 0.0145$, $R^2 = 0.7562$). Tukey's post-hoc comparison showed that SOX4

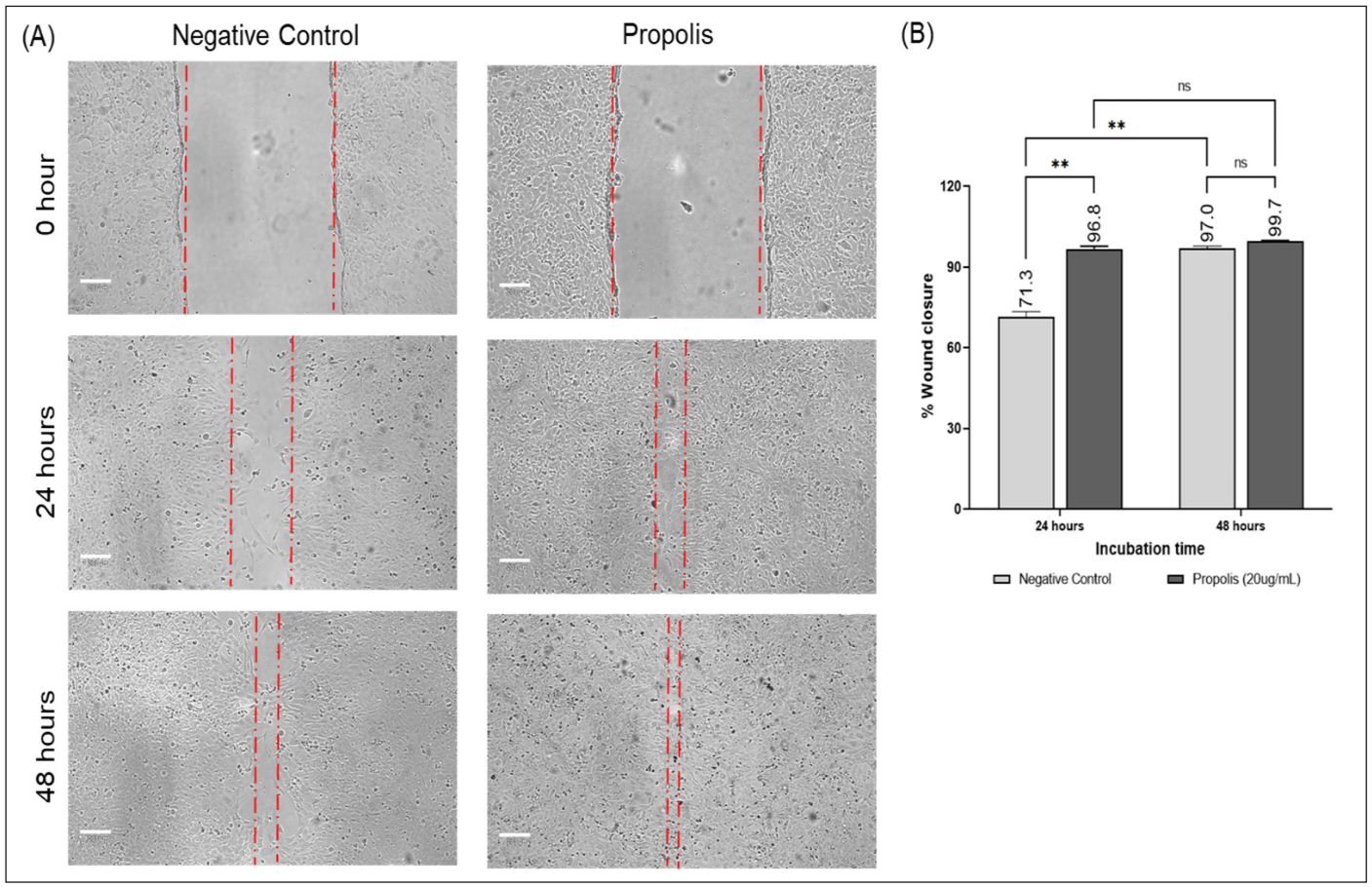

Figure 5. Wound closure of the 1306 fibroblast cell line after treatment with 20 µg/ml propolis at 24 and 48 hours of observation. (A) Representative images of the scratch area (wound width) over time. (B) Quantification of the percentage (%) of wound closure. Data are presented as mean ± SD. ns = not significant; ** = $p < 0.01$.

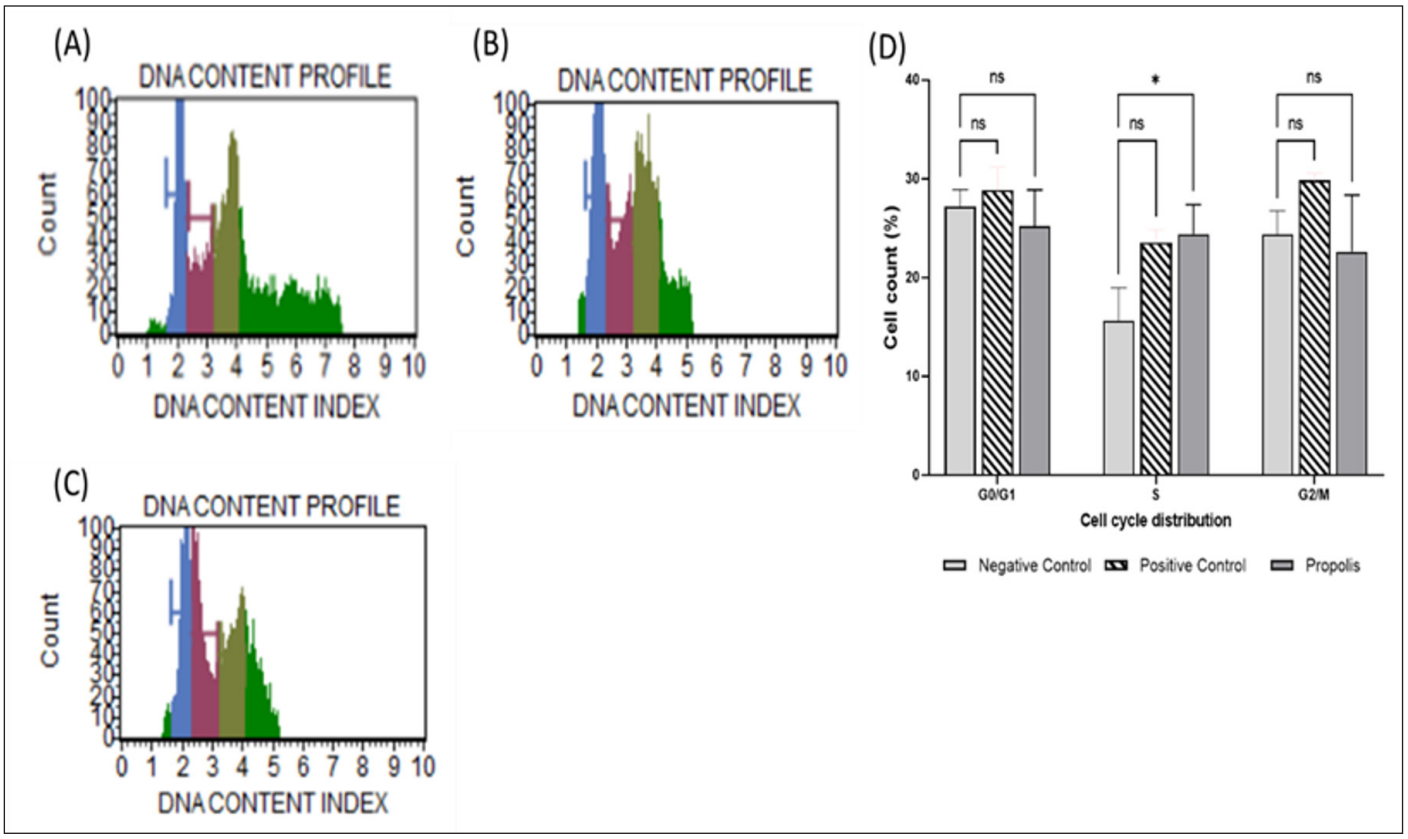

Figure 6. Cell cycle distribution analysis via flow cytometry. Distribution of 1306 human skin fibroblasts after 48 hours of treatment. (A) Negative control; (B) Positive control (insulin); (C) Cells treated with 20 µg/ml propolis; (D) Quantitative analysis of cell populations in G0/G1, S, and G2/M phases. Data represent mean ± SD. ns = not significant; * = $p < 0.05$.

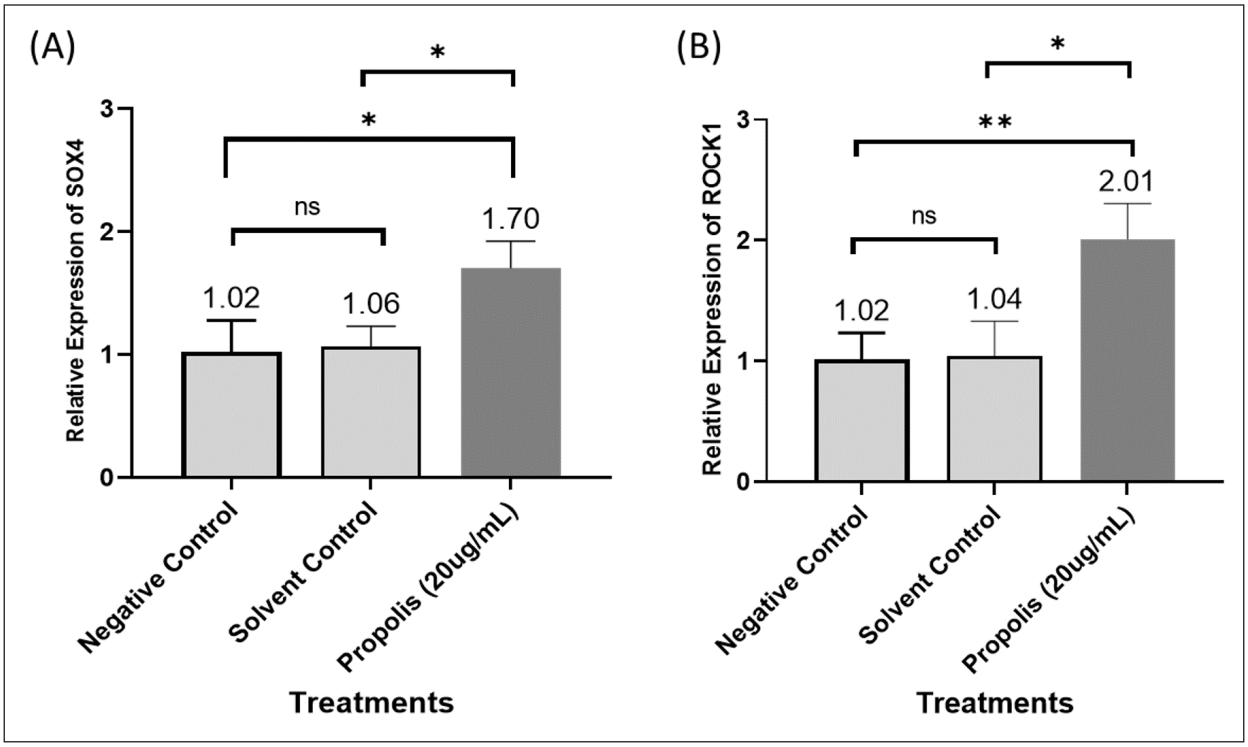

Figure 7. Relative expression of the target gene after treatment with 20 µg/ml propolis. (A) SOX4 relative expression; (B) ROCK1 relative expression in 1306 fibroblasts treated with 20 µg/ml propolis. mRNA levels were normalized to GAPDH using the $2^{-\Delta\Delta Cq}$ method. Values above each bar indicate the group mean of relative expression. Data are shown as mean ± SD. ns = not significant; * = $p < 0.05$; ** = $p < 0.01$.

expression was significantly higher in the propolis-treated group compared to the negative control (mean difference = 0.6797, 95% CI: 0.1370 to 1.222, $p = 0.0200$) and compared to the solvent control (mean difference = 0.6400, 95% CI: 0.0974 to 1.183, $p = 0.0258$), while the negative and solvent controls did not differ significantly from each other ($p = 0.9728$). Similarly, one-way ANOVA revealed a significant effect of treatment on ROCK1 mRNA expression ($F(2,6) = 13.11$, $p = 0.0065$, $R^2 = 0.8138$). ROCK1 expression was significantly higher in the propolis-treated group compared to the negative control (mean difference = 0.9957, 95% CI: 0.3152 to 1.676, $p = 0.0099$) and compared to the solvent control (mean difference = 0.9710, 95% CI: 0.2905 to 1.651, $p = 0.0111$), while the negative and solvent controls did not differ significantly from each other ($p = 0.9932$). These findings suggested that propolis treatment upregulated the mRNA expression levels of both SOX4 and ROCK1 in 1306 fibroblast cells relative to control conditions.

4. DISCUSSION

Propolis has a long history of use in natural and complementary medicine for treating topical wounds and chronic ulcers, a performance largely attributed to its local anesthetic and antiseptic characteristics. It is widely accepted that the clinical benefits of propolis are driven by its dense concentration of active flavonoids. Propolis ethanolic extract exhibited an IC_{50} of 51.08 µg/ml, which represents moderate radical-scavenging activity (Fig. 1). This aligns with the classification by Phongpaichit *et al.* [25], who defined IC_{50} values of 50–100 µg/ml as moderately active. The inclusion of flavonoid molecules with hydroxyl groups is responsible for propolis's modest free radical inhibitory action. These hydroxyl groups serve as the active moieties (or active sites) that react with the DPPH radicals [26,27]. In this study, HPLC analysis tentatively indicated the presence of quercetin in the propolis extract (Fig. 2). This finding aligns with previous studies, which have identified quercetin in propolis samples from various geographical origins, including India, Morocco, Palestine, Timis County, Turkey, Poland, Azerbaijan, and Kediri [21,22,28–31].

Quercetin is a natural flavonoid ubiquitously found in the plant kingdom [32]. It has a diverse range of pharmacological effects, such as anti-inflammatory [32], anti-senescence [33,34], anti-neoplastic [35], and antioxidant [36] functions. Furthermore, quercetin is a good candidate chemical for hastening the healing of skin wounds, according to current research [32].

While some studies highlighted the anti-cancer properties of propolis [20,23], recent evidence demonstrates that at specific non-toxic doses, propolis can enhance cell viability, proliferation, migration, and target gene expression in fibroblasts, serving as an effective in vitro model for wound healing [37,38]. This is critical because fibroblasts are the primary cellular engines driving skin repair via coordinated migration and mitotic expansion [39]. Our findings align with those of research showing that propolis induces cell viability at specific concentrations (20 and 40 µg/ml) but becomes cytotoxic to the fibroblast cell line at concentrations exceeding 40 µg/ml (Fig. 3).

Based on the results, propolis accelerated wound closure significantly compared with the negative control. This enhanced wound closure may be partly attributable to quercetin, one of several bioactive constituents present in the propolis extract, although the relative contribution of quercetin versus other, uncharacterized propolis constituents cannot be determined from the present targeted HPLC analysis. Previous research by Doersch and Newell-Rogers [40] demonstrated that quercetin interacts with β-integrins, thereby influencing the wound-healing pathways. Quercetin has been reported to increase TGF-β1 expression in rodent cutaneous wound models, alongside enhanced fibroblast proliferation and collagen deposition [41], and TGF-β signaling has separately been reported to activate ROCK1 [42–44]. Whether this axis operates in the present model was not tested here.

ROCK proteins function as essential regulators of the cytoskeleton. Literature suggests that fibroblast movement requires intracellular signaling changes mediated by the ROCK/Rho pathway [45]. Increased ROCK1 expression has been reported to facilitate FAK phosphorylation and thereby promote cell motility, although ROCK1 was measured here only at the mRNA level and neither ROCK1 protein nor kinase activity was assessed [45,46]. These reports are consistent with the present findings, in which significant upregulation of ROCK1 (Fig. 7B) was accompanied by accelerated wound closure (Fig. 5).

In addition, the fibroblast cell line exhibited increased wound closure capacity, which may also involve increased cell number. Our analysis indicated that propolis treatment shifted the cell cycle of the repairing fibroblasts from the G0/G1 phase to the S phase, suggesting an enhanced proliferative capacity in propolis-treated cells. In view of this shift in cell cycle distribution, we further evaluated the expression of SOX4, a transcription factor reported to regulate cell cycle progression. Treatment with 20 µg/ml propolis demonstrated a significant increase in SOX4 mRNA expression (Fig. 7A), consistent with a possible role for SOX4 in fibroblast proliferation that remains to be functionally confirmed. It should be noted that SOX4 activity is context-dependent: while transient upregulation supports fibroblast proliferation and tissue repair, sustained or dysregulated SOX4 expression has been associated with fibroblast-to-myofibroblast transition, fibrosis, and tumourigenesis. As the present study evaluated SOX4 expression at a single time point, whether the observed induction is transient or sustained remains undetermined; time-course analysis is recommended in future work. A propolis-derived flavonoid, pinocembrin, has been reported to interact with SOX4 and to modulate its dysregulated expression in a murine arthritis model [47], indicating that propolis constituents can engage this transcription factor; the direction of that effect in fibroblasts, however, has not been established.

SOX4 belongs to the HMG-box family and plays a central role in tissue development. Previous studies found that the overexpression of SOX4 in mammalian cells promotes migration, invasion, and epithelial-mesenchymal transition processes. Smith *et al.* [48] further explained that SOX4 significantly improves the reprogramming of human fibroblasts and glioblastoma cells by promoting chromatin remodeling. SOX4 stabilizes intracellular β-catenin, thereby amplifying downstream β-catenin/TCF signaling. Lee *et al.* [49] found that SOX4 causes a dose-dependent increase in β-catenin accumulation and upregulates its direct mitogenic target, Cyclin D1.

These mechanisms elucidate the findings of the current study, which showed a significant expansion of the fibroblast population within the S phase compared to controls (Fig. 6). This increase is consistent with more rapid cell cycle progression, alongside the increased cell viability observed 24 hours after treatment, as shown in Figure 4. Based on these findings, this study suggests that propolis treatment is associated with two phenotypic changes relevant to wound healing: increased cell viability with S-phase entry and accelerated wound closure, accompanied by upregulation of SOX4 and ROCK1 transcripts.

While propolis-induced fibroblast viability and wound closure have been reported previously, the present study contributes on two distinct fronts. First, the material examined here is a stingless bee (*Trigona* sp.) propolis of West Javanese origin. Stingless bee propolis

differs chemically from European honeybee propolis on which most fibroblast wound-healing studies are based, and propolis composition varies with geographical and botanical source; data on Indonesian *Trigona* sp. material in a human dermal fibroblast model therefore cannot be assumed from the existing literature. This extract was characterized across a single internally consistent panel of endpoints, comprising a graded cytotoxicity screen that defined the non-toxic range, cell viability, wound closure, cell cycle distribution and target gene expression, all at one non-toxic concentration established within the same cell model. Second, the study identifies SOX4 and ROCK1 transcriptional upregulation as candidate molecular correlates of these phenotypic responses, an association not previously described for propolis. SOX4 has an established, functionally validated role in cell cycle regulation [11] and ROCK1 in fibroblast contractility [12], yet neither has been examined as a transcriptional correlate of propolis-induced fibroblast activation. We present this as an incremental, hypothesis-generating contribution rather than a demonstrated mechanism. The transcriptional changes reported here are modest (1.70-fold for SOX4 and 2.01-fold for ROCK1) and were not accompanied by protein-level or functional validation. Their value lies in narrowing a chemically complex extract and a set of phenotypic observations to two specific, independently validated candidates that can be tested directly by knockdown, rescue, and protein-level approaches in future work.

The scope of the present design should be stated explicitly. Experiments were conducted in the non-diabetic 1306 dermal fibroblast line, so the findings characterize propolis activity in a transformed human fibroblast cell line model and are not directly extrapolable to the diabetic condition emphasized in the Introduction; a diabetic or high-glucose-induced model is the appropriate next step. Functional endpoints were evaluated at the single non-toxic concentration (20 µg/ml) selected from the cytotoxicity screen, and responses at the remaining non-toxic concentration (40 µg/ml) were not examined. Chemical characterization by HPLC targeted quercetin as a representative marker; propolis is a chemically complex matrix containing numerous other constituents (e.g., pinocembrin, galangin), and broader profiling (e.g., LC-MS/MS) would be required to determine their relative contributions. The material was identified at genus level (*Trigona* sp.); species-level identification, collection period, batch number, botanical origin, extraction yield, and storage conditions were not systematically documented, which constrains cross-study comparability of the extract.

Three constraints bound the interpretation offered here. First, the association between the observed phenotypes and SOX4/ROCK1 expression rests on transcriptional data alone; no protein-level (e.g., Western blot) or functional validation (e.g., siRNA knockdown or rescue) was performed, and the association is therefore correlative rather than causal. Second, because MTT reports cellular metabolic activity rather than cell number directly, the increase in absorbance may reflect enhanced metabolic activity rather than a proportional increase in cell number; EdU/BrdU incorporation or Ki-67 staining would be required to confirm proliferation specifically. Third, the scratch assay was performed without a proliferation-blocking agent (e.g., mitomycin C) and therefore reports wound closure rather than migration alone. Mycoplasma testing was not performed, although routine antibiotic-antimycotic supplementation was used during culture, and melt-curve data were not available to independently confirm amplicon specificity. These constraints define the boundaries of the mechanistic claims that can be drawn at present; they do not affect the phenotypic observations themselves, which were consistent across the panel of endpoints examined.

5. CONCLUSION

This study showed that propolis significantly enhanced the viability and wound closure of the 1306 human skin fibroblast cell line compared to the negative control. These stimulatory effects were observed following treatment with 20 µg/ml propolis. Our findings revealed that enhanced cell viability and wound closure were associated with the upregulation of SOX4 and ROCK1 mRNA expression. These mRNA expression profiles suggest a potential involvement of these genes in the observed cellular responses. The ability of propolis (20 µg/ml) to simultaneously enhance cell viability, S-phase entry, and wound closure in fibroblasts, alongside upregulation of SOX4 and ROCK1 transcripts, supports its potential as a candidate wound-healing agent warranting further mechanistic (protein-level and functional) validation and evaluation in disease-relevant, including diabetic, fibroblast models before translational claims can be made.

6. ACKNOWLEDGMENT

The researcher would like to thank Agres Oktaviani, S.Si, and Hesti Famella Ahsani Nissa, S. Si, who assisted with the instrumentation facilities during the research.

7. AUTHOR CONTRIBUTIONS

All authors made substantial contributions to conception and design, acquisition of data, or analysis and interpretation of data; took part in drafting the article or revising it critically for important intellectual content; agreed to submit the article to the current journal; gave final approval of the version to be published; and agree to be accountable for all aspects of the work. All the authors are eligible to be authors as per the International Committee of Medical Journal Editors (ICMJE) requirements/guidelines.

8. ETHICS APPROVAL

This study involved no human participants, human tissue samples, or animal subjects. All experimental work was performed *in vitro* using an established commercial fibroblast cell line. No ethical approval was sought or required, and the authors confirm that this study involves no ethical issues.

9. CONFLICTS OF INTEREST

The authors report no financial or any other conflicts of interest in this work.

10. DATA AVAILABILITY

All the data is available with the authors and shall be provided upon request.

11. FUNDING

There is no funding to report.

12. PUBLISHER'S NOTE

All claims expressed in this article are solely those of the authors and do not necessarily represent those of the publisher, the editors, and the reviewers. This journal remains neutral with regard to jurisdictional claims in published institutional affiliation.

13. USE OF ARTIFICIAL INTELLIGENCE (AI)-ASSISTED TECHNOLOGY

The authors declare that they have not used artificial intelligence (AI) tools for writing and editing of the manuscript, and no images were manipulated using AI.

REFERENCES

1. Fernandez-Guarino M, Naharro-Rodriguez J, Bacci S. Aberrances of the wound healing process: a review. Cosmetics 2024;11(6):1–22; doi: https://doi.org/10.3390/cosmetics11060209
2. Sun H, Saeedi P, Karuranga S, Pinkepank M, Ogurtsova K, Duncan BB, *et al.* IDF Diabetes Atlas: global, regional and country-level diabetes prevalence estimates for 2021 and projections for 2045. Diabetes Res Clin Pract 2022;183:1–23; doi: https://doi.org/10.1016/j.diabres.2021.109119
3. Dasari N, Jiang A, Skochdopole A, Chung J, Reece EM, Vorstenbosch J, *et al.* Updates in diabetic wound healing, inflammation, and scarring. Semin Plast Surg 2021;35(3):153–8; doi: https://doi.org/10.1055/s-0041-1731460
4. Armstrong DG, Boulton AJM, Bus SA. Diabetic foot ulcers and their recurrence. N Engl J Med 2017;376(24):2367–75; doi: https://doi.org/10.1056/nejmra1615439
5. Vu DM, Nguyen VT, Nguyen TH, Do PTX, Dao HH, Hai DX, *et al.* Effects of extracellular vesicles secreted by TGFβ-stimulated umbilical cord mesenchymal stem cells on skin fibroblasts by promoting fibroblast migration and ECM protein production. Biomedicines 2022;10(8):1–12; doi: https://doi.org/10.3390/biomedicines10081810
6. Desjardins-Park HE, Foster DS, Longaker MT. Fibroblasts and wound healing: an update. Regen Med 2018;13(5):491–5; doi: https://doi.org/10.2217/rme-2018-0073
7. El-Sakhawy M, Salama A, Tohamy HAS. Applications of propolis-based materials in wound healing. Arch Dermatol Res 2024;316(1):1–3; doi: https://doi.org/10.1007/s00403-023-02789-x
8. Plikus MV, Wang X, Sinha S, Forte E, Thompson SM, Herzog EL, *et al.* Fibroblasts: origins, definitions, and functions in health and disease. Cell 2021;184(15):3852–72; doi: https://doi.org/10.1016/j.cell.2021.06.024
9. Knoedler S, Broichhausen S, Guo R, Dai R, Knoedler L, Kauke-Navarro M, *et al.* Fibroblasts—the cellular choreographers of wound healing. Front Immunol 2023;14:1–6; doi: https://doi.org/10.3389/fimmu.2023.1233800
10. Cialdai F, Risaliti C, Monici M. Role of fibroblasts in wound healing and tissue remodeling on Earth and in space. Front Bioeng Biotechnol 2022;10:1–8; doi: https://doi.org/10.3389/fbioe.2022.958381
11. Sun R, Jiang B, Qi H, Zhang X, Yang J, Duan J, *et al.* SOX4 contributes to the progression of cervical cancer and the resistance to the chemotherapeutic drug through ABCG2. Cell Death Dis 2015;6:e1990; doi: https://doi.org/10.1038/cddis.2015.290
12. Hallgren O, Rolandsson S, Andersson-Sjöland A, Nihlberg K, Wieslander E, Kvist-Reimer M, *et al.* Enhanced ROCK1 dependent contractility in fibroblast from chronic obstructive pulmonary disease patients. J Transl Med 2012;10:171; doi: https://doi.org/10.1186/1479-5876-10-171
13. Ayad AS, Benchaabane S, Daas T, Smagghe G, Loucif-Ayad W. Propolis stands out as a multifaceted natural product: meta-analysis on its sources, bioactivities, applications, and future perspectives. Life 2025;15(5):1–44; doi: https://doi.org/10.3390/life15050764
14. Dekebo A, Geba C, Bisrat D, Jeong JB, Jung C. Wound Healing, Anti-Inflammatory and Anti-Oxidant Activities, and Chemical Composition of Korean Propolis from Different Sources. Int J Mol Sci 2024;25(21):11352; doi: https://doi.org/10.3390/ijms252111352
15. Ernawati D, Puspasari A, Harijanti K, Soebadi B, Hendarti H, Radithia D. Effects of topical application of propolis extract on fibroblast growth factor-2 and fibroblast expression in the traumatic ulcers of diabetic Rattus norvegicus. J Oral Maxillofacial Pathol 2018;22(1):54–8; doi: https://doi.org/10.4103/jomfp.JOMFP_82_17
16. Sungkar A, Doewes M, Purwanto B, Wasita B. The effect of Indonesian propolis dosage on vascularization of skin graft in skin wound of white rat's skin graft model: molecular studies of malondialdehyde (mda), nuclear factor-kappa beta (nf-kb), interleukin-6, vascular endothelial growth factor (VEGF), caspase-3, and microvessels density (MVD) Bali Med J 2021;10(2):811–20; doi: https://doi.org/10.15562/bmj.v10i2.2339
17. Hozzein WN, Badr G, Al Ghamdi AA, Sayed A, Al-Waili NS, Garraud O. Topical application of propolis enhances cutaneous wound healing by promoting TGF-beta/Smad-mediated collagen production in a streptozotocin-induced type I diabetic mouse model. Cell Physiol Biochem 2015;37(3):940–54; doi: https://doi.org/10.1159/000430221
18. Zomer HD, Trentin AG. Skin wound healing in humans and mice: challenges in translational research. J Dermatol Sci 2018;90(1):3–12; doi: https://doi.org/10.1016/j.jdermsci.2017.12.009
19. Popova M, Trusheva B, Bankova V. Propolis of stingless bees: a phytochemist's guide through the jungle of tropical biodiversity. Phytomedicine 2021;86:153098; doi: https://doi.org/10.1016/j.phymed.2019.153098
20. Tan MI, Rahayu AK. Synthesis of chitosan-folic acid nanoparticles as a drug delivery system for propolis compounds. In: Amid A. (eds.). Multifaceted protocols in biotechnology, Springer, Cham, Switzerland, Volume 2, pp 145–59, 2021; doi: https://doi.org/10.1007/978-3-030-75579-9_10
21. Kurek-Górecka A, Kara Y, Pokajewicz K, Ben Hammouda I, Wieczorek PP, Marciniak D, *et al.* Phenolic content, volatile compounds and antioxidant activity in pooled propolis samples from Turkey and Poland. Eur Food Res Technol 2025;251(8):2199–210; doi: https://doi.org/10.1007/s00217-025-04756-4
22. Can Z, Yildiz O, Şahin H, Asadov E, Kolayli S. Phenolic profile and antioxidant potential of propolis from Azerbaijan. Mellifera 2015;15(1):14–8.
23. Adhika OA, Rahayu AK, Jonathan T, Gunadi JW. Effect of propolis on inhibiting the proliferation and migration of T47D breast cancer cell lines. Glob Med Health Commun 2025;13(2):93–101; doi: https://doi.org/10.29313/gmhc.v13i2.7732
24. Rahayu AK, Fibriani A, Tan MI. Exploring the potential of black cumin derived nanovesicles for miRNA drug delivery. Eur J Pharm Biopharm 2024;199: 114275; doi: https://doi.org/10.1016/j.ejpb.2024.114275
25. Phongpaichit S, Nikom J, Rungjindamai N, Sakayaroj J, Hutadilok-Towatana N, Rukachaisirikul V, *et al.* Biological activities of extracts from endophytic fungi isolated from Garcinia plants. FEMS Immunol Med Microbiol 2007;51(3):517–25; doi: https://doi.org/10.1111/j.1574-695X.2007.00331.x
26. Jun M. Comparison of antioxidant activities of isoflavones from kudzu root (*Pueraria lobata* Ohwi). J Food Sci 2003;68(6):2117–22; doi: https://doi.org/10.1111/j.1365-2621.2003.tb07029.x
27. Alvarez-Suarez JM, editor. Bee products: chemical and biological properties. 1st ed. Cham, Switzerland: Springer; 2017. 306 p; doi: https://doi.org/10.1007/978-3-319-59689-1
28. Thirugnanasampandan R, Raveendran SB, Jayakumar R. Analysis of chemical composition and bioactive property evaluation of Indian propolis. Asian Pac J Trop Biomed 2012;2(8):651–4; doi: https://doi.org/10.1016/S2221-1691(12)60114-2
29. Touzani S, Imtara H, Katekhaye S, Mechchate H, Ouassou H, Alqahtani AS, *et al.* Determination of phenolic compounds in various propolis samples collected from an African and an Asian region and their impact on antioxidant and antibacterial activities. Molecules 2021;26(15):4589; doi: https://doi.org/10.3390/molecules26154589
30. Heghedus-Mindru RC, Heghedus-Mindru G, Stef DS. Identification of Quercetin and Rutin from Propolis Ethanolic Extract (EEP) of Timis County [Internet]. Scientific Papers Anim Sci & Biotechnologies / Lucrari Stiintifice Zootehnie Si Biotehnologii 2015;48(1):123–7; Available via http://search.ebscohost.com/login.aspx?direct=true&db=asn&AN=108532152&site=ehost-live
31. Kusnul Z, Puspita E, Azizah U, Rifai M. Identification and quantification of propolis's active compound in various solvents. J Appl Environ Biol Sci 2016;6(9):94–9.
32. Wu D, Jiang M, Zhang J. Dual Role of Quercetin in Promoting Early Wound Healing via Inhibiting Inflammatory Factors and Attenuating Scar Formation by Suppressing Myofibroblast Differentiation.

Front Biosci (Landmark Ed) 2025;30(7):40077; doi: https://doi.org/10.31083/FBL40077
33. Yang Y, Li Y, Du X, Liu Z, Zhu C, Mao W, *et al.* Anti-Aging Effects of Quercetin in Cladocera Simocephalus vetulus Using Proteomics. ACS Omega 2023;8(20):17609–19; doi: https://doi.org/10.1021/acsomega.2c08242
34. Chondrogianni N, Kapeta S, Chinou I, Vassilatou K, Papassideri I, Gonos ES. Anti-ageing and rejuvenating effects of quercetin. Exp Gerontol 2010;45(10):763–71; doi: https://doi.org/10.1016/j.exger.2010.07.001
35. Shahbaz M, Naeem H, Momal U, Imran M, Alsagaby SA, Al Abdulmonem W, *et al.* Anticancer and apoptosis inducing potential of quercetin against a wide range of human malignancies. Int J Food Prop 2023;26(1):2590–626; doi: https://doi.org/10.1080/10942912.2023.2252619
36. Qi W, Qi W, Xiong D, Long M. Quercetin: its antioxidant mechanism, antibacterial properties and potential application in prevention and control of toxipathy. Molecules 2022;27(19): 6545; doi: https://doi.org/10.3390/molecules27196545
37. Ebadi P, Fazeli M. Evaluation of the potential *in vitro* effects of propolis and honey on wound healing in human dermal fibroblast cells. S Afr J Bot 2021;137:414–22; doi: https://doi.org/10.1016/j.sajb.2020.10.003
38. Jongjitaree S, Koontongkaew S, Niyomtham N, Yingyongnarongkul BE, Utispan K. The oral wound healing potential of thai propolis based on its antioxidant activity and stimulation of oral fibroblast migration and proliferation. Evidence-based Complementary Alternative Med 2022;2022:3503164; doi: https://doi.org/10.1155/2022/3503164
39. Schäfer M, Werner S. Transcriptional control of wound repair. Annu Rev Cell Dev Biol 2007;23:69–92; doi: https://doi.org/10.1146/annurev.cellbio.23.090506.123609
40. Doersch KM, Newell-Rogers MK. The impact of quercetin on wound healing relates to changes in αV and β1 integrin expression. Exp Biol Med 2017;242(14):1424–31; doi: https://doi.org/10.1177/1535370217712961
41. Gopalakrishnan A, Ram M, Kumawat S, Tandan S, Kumar D. Quercetin accelerated cutaneous wound healing in rats by increasing levels of VEGF and TGF-β1. Indian J Exp Biol 2016;54(3):187–95.
42. Shimada H, Staten NR, Rajagopalan LE. TGF-β1 mediated activation of Rho kinase induces TGF-β2 and endothelin-1 expression in human hepatic stellate cells. J Hepatol 2011;54(3):521–8; doi: https://doi.org/10.1016/j.jhep.2010.07.026
43. Bu DX, Rai V, Shen X, Rosario R, Lu Y, D'Agati V, *et al.* Activation of the ROCK1 branch of the transforming growth factor-β pathway contributes to RAGE-dependent acceleration of atherosclerosis in diabetic ApoE-Null mice. Circ Res 2010;106(6):1040–51; doi: https://doi.org/10.1161/CIRCRESAHA.109.201103
44. Li Y, Li J, Zhou L, Wang Z, Jin L, Cao J, *et al.* Aberrant activation of TGF-β/ROCK1 enhances stemness during prostatic stromal hyperplasia. Cell Commun Signal 2024;22(1):1–19; doi: https://doi.org/10.1186/s12964-024-01644-4
45. Jackson BT, Artlett CM. Fibroblast migration in fibrosis. Fibrosis 2025;3(2):10009; doi: https://doi.org/10.70322/fibrosis.2025.10009
46. Hu C, Zhou H, Liu Y, Huang J, Liu W, Zhang Q, *et al.* ROCK1 promotes migration and invasion of non-small-cell lung cancer cells through the PTEN/PI3K/FAK pathway. Int J Oncol 2019;55(4):833–44; doi: https://doi.org/10.3892/ijo.2019.4864
47. Ahmed EA, Ibrahim HIM, Khalil HE. Pinocembrin reduces arthritic symptoms in mouse model via targeting Sox4 signaling molecules. J Med Food 2021;24(3):282–91; doi: https://doi.org/10.1089/jmf.2020.4862
48. Smith DK, Yang J, Liu ML, Zhang CL. Small molecules modulate chromatin accessibility to promote NEUROG2-mediated fibroblast-to-neuron reprogramming. Stem Cell Rep 2016;7(5):955–69; doi: https://doi.org/10.1016/j.stemcr.2016.09.013
49. Lee AK, Ahn SG, Yoon JH, Kim SA. Sox4 stimulates β-catenin activity through induction of CK2. Oncol Rep 2011;25(2):559–65; doi: https://doi.org/10.3892/or.2010.1091

How to cite this article:
Herdiman MH, Rahayu AK, Gunadi JW. Propolis enhances fibroblast wound healing behavior and is associated with upregulation of SOX4 and ROCK1 mRNA expression. J Appl Biol Biotech 2027;15(1):149-160. DOI: 10.7324/jabb.2026.325946